

Improved constraints on 21st-century warming derived using 160 years of temperature observations

N. P. Gillett,¹ V. K. Arora,¹ G. M. Flato,¹ J. F. Scinocca,¹ and K. von Salzen¹

Received 4 November 2011; accepted 28 November 2011; published 10 January 2012.

[1] Projections of 21st century warming may be derived by using regression-based methods to scale a model's projected warming up or down according to whether it under- or over-predicts the response to anthropogenic forcings over the historical period. Here we apply such a method using near surface air temperature observations over the 1851–2010 period, historical simulations of the response to changing greenhouse gases, aerosols and natural forcings, and simulations of future climate change under the Representative Concentration Pathways from the second generation Canadian Earth System Model (CanESM2). Consistent with previous studies, we detect the influence of greenhouse gases, aerosols and natural forcings in the observed temperature record. Our estimate of greenhouse-gas-attributable warming is lower than that derived using only 1900–1999 observations. Our analysis also leads to a relatively low and tightly-constrained estimate of Transient Climate Response of 1.3–1.8°C, and relatively low projections of 21st-century warming under the Representative Concentration Pathways. Repeating our attribution analysis with a second model (CNRM-CM5) gives consistent results, albeit with somewhat larger uncertainties. **Citation:** Gillett, N. P., V. K. Arora, G. M. Flato, J. F. Scinocca, and K. von Salzen (2012), Improved constraints on 21st-century warming derived using 160 years of temperature observations, *Geophys. Res. Lett.*, *39*, L01704, doi:10.1029/2011GL050226.

1. Introduction

[2] Quantitative comparisons of simulated and observed temperature changes over past decades not only help determine the causes of observed changes, but also may be used as a constraint on simulated projections of future change. Allen *et al.* [2000] and Kettleborough *et al.* [2007] demonstrated that there is close to a linear relationship between the simulated warming over the historical period and that in the 21st century in energy balance models with a range of climate sensitivity and ocean heat uptake coefficients, at least for scenarios with progressively increasing radiative forcing. This means that if a climate model overpredicts past greenhouse-gas-induced warming, then it is expected to also overpredict future greenhouse-gas-induced warming, and this effect may be corrected by multiplying projected changes by a scaling factor derived from past changes. Moreover the uncertainties in the derived projection may be estimated from observational constraints, providing a proba-

bilistic projection whose uncertainties are not determined from a spread in projections across an ad-hoc ensemble of climate models.

[3] Studies assessed by Meehl *et al.* [2007] constrained projections using observations only over the period 1900–1999, and projected ranges of warming were generally at least as wide as those derived from the ensemble spread of the CMIP3 models. However, reliable surface temperature observations extend back to 1850, and even though spatial coverage has increased through time, uncertainty in decadal timescale global mean temperature in the period 1850–1900 was no larger than that in the early part of the 20th century, since bias uncertainties were particularly large in the early 20th century [Brohan *et al.*, 2006]. Further we now have an additional eleven years of surface temperature observations (2000–2010), over a period in which anthropogenic forcing has been larger than ever before, which is expected to reduce uncertainties [Stott and Kettleborough, 2002]. The inclusion of more data from the period since 1990 in which the aerosol forcing has decreased should also make the aerosol and greenhouse gas responses less degenerate.

[4] In this study we use new historical simulations and Representative Concentration Pathway (RCP) [Moss *et al.*, 2010] scenario simulations from CanESM2 firstly to derive scaling factors on the greenhouse gas and aerosol forcing responses which give the best fit to observations over the historical period, and then to derive observationally-constrained projections of 21st-century temperature change.

2. Model and Simulations

[5] CanESM2 is the latest generation Canadian coupled ocean-atmosphere model, including an interactive carbon cycle [Arora *et al.*, 2011]. The model also includes an interactive sulphur cycle, and represents the effect of sulphate aerosol on cloud brightness. We use 1280 years of control simulation, with constant preindustrial forcings including constant specified CO₂, and a five-member ensemble of historical simulations from 1850–2005 including prescribed historical greenhouse gas concentrations, SO₂ and other aerosol-precursor emissions, land use changes, solar irradiance changes, tropospheric and stratospheric ozone changes, and volcanic aerosol (ALL), following the recommended CMIP5 specifications (<http://cmip-pcmdi.llnl.gov/cmip5/forcing.html>). We also use five-member ensembles of simulations with greenhouse gas changes only (GHG), volcanic and solar irradiance changes only (NAT), and aerosol changes only (AER) over the period 1850–2010. We use five-member ensembles of scenario simulations from 2006–2100 with RCP 2.6, RCP 4.5, and RCP 8.5 [Moss *et al.*, 2010] changes in greenhouse gases and aerosol precursor emissions, projected ozone changes, and a repeated solar

¹Canadian Centre for Climate Modelling and Analysis, Environment Canada, Victoria, British Columbia, Canada.

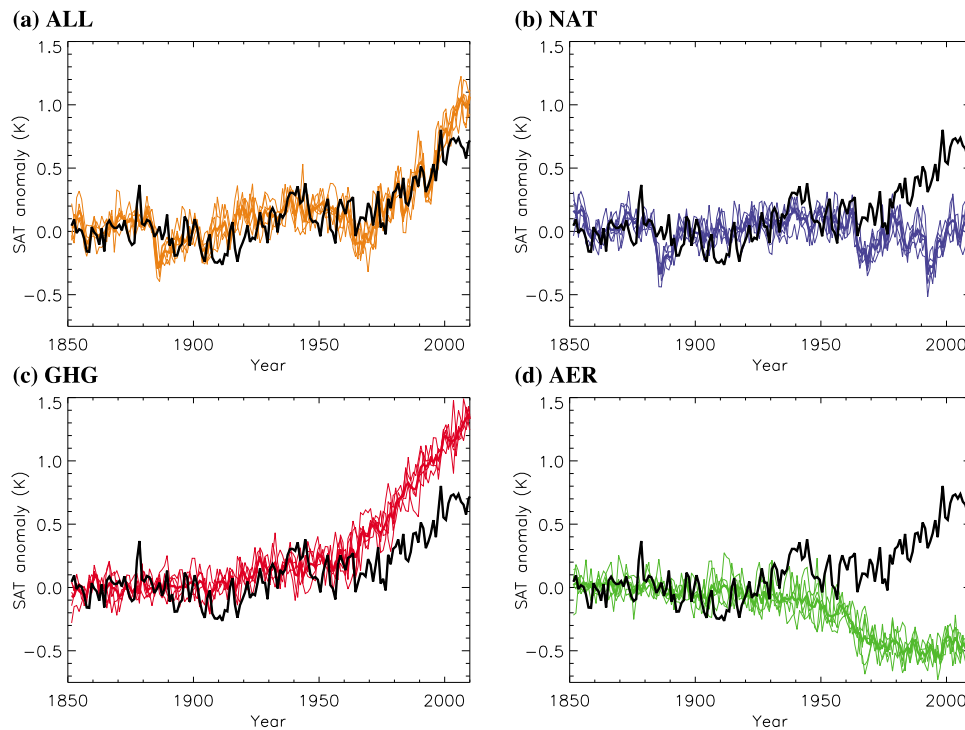


Figure 1. Time series of global mean near-surface air temperature anomalies in observations and simulations of CanESM2. Black lines show observed global mean annual mean temperature from HadCRUT3, and thin coloured lines show global mean temperature from five-member ensembles of CanESM2 forced with (a) anthropogenic and natural forcings (ALL), (b) natural forcings only (NAT), (c) greenhouse gases only (GHG), and (d) aerosols only (AER). All anomalies are calculated relative to the period 1851–1900, and ensemble means are shown by thick coloured lines.

cycle, also following recommended CMIP5 specifications. We additionally use three five-member ensembles of simulations from 2006–2100 with projected greenhouse gas changes only from each RCP. Output from each historical ALL simulation was merged with output from the corresponding RCP 4.5 simulation for the period 2006–2010, to give simulations over the full period 1850–2010. Radiative forcing differs negligibly between RCPs over the period 2006–2010 [Moss *et al.*, 2010], and is likely to have been close to the actual forcing over this period.

3. Results

[6] Figure 1a compares observed HadCRUT3 [Brohan *et al.*, 2006] global mean temperature with that simulated in response to anthropogenic and natural forcing by CanESM2, where model output was masked with the observational coverage. The model broadly captures the variations in global mean temperature observed over the past 160 years, with warming in the early 20th century, relatively constant temperatures through the middle part of the century, and strong warming since 1970. In the model, the slight cooling simulated in ALL between 1940 and 1970 is related to a large tropospheric-aerosol-induced cooling (Figure 1d), and stratospheric-aerosol-induced cooling following the 1961 Agung eruption (Figure 1b), while the increased rate of warming since around 1970 is driven by an increased rate of greenhouse-gas-induced warming coupled with little change in aerosol response (Figure 1c). Pronounced cooling is simulated in response to explosive volcanic eruptions (Figure 1b), in particular after Krakatoa (1883), Agung

(1963), and Pinatubo (1991). Cooling is apparent in the observations after the eruptions of Pinatubo and Agung, but it appears to be weaker than that simulated, and little or no cooling was observed after Krakatoa: The CMIP3 models also overestimate the cooling following Krakatoa, and *Joshi and Jones* [2009] suggest that this may be due to a large injection of stratospheric water vapour during this eruption which is not included in climate model simulations. Comparing the warming over the whole period in Figure 1a, there is some evidence that the model appears to warm more than the observations, primarily due to differences in the final decade.

[7] As in observations (Figure 2a), the ALL simulations of CanESM2 (Figure 2b) show warming almost everywhere over the 1851–2010 period. However, while the simulated trends are somewhat larger than observed over much of the Southern Hemisphere and tropics, the simulated warming is much weaker than observed over most of the Northern Hemisphere mid- and high-latitude continents. This is due to strong aerosol-induced cooling in the model (Figure 2d), which cancels out much of the greenhouse-gas-induced warming in these regions (Figure 2c). These results suggest that the aerosol-induced cooling may be somewhat too strong in the model.

[8] In order to quantitatively compare simulated and observed temperature changes we apply a detection and attribution analysis following *Huntingford et al.* [2006], *Stott et al.* [2006] and *Hegerl et al.* [2007]. As well as greenhouse gas and aerosol forcing changes, the ALL simulations include land use changes and stratospheric and tropospheric ozone changes. In order to account for all the

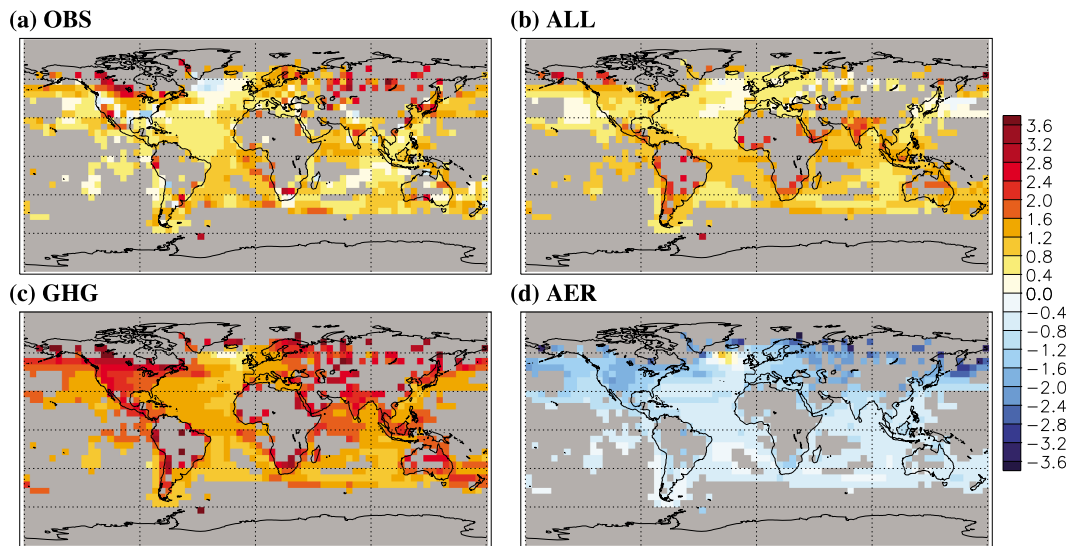


Figure 2. Near-surface air temperature trends in $^{\circ}\text{C}$ over the 160-year period 1851–2010 in (a) HadCRUT3 observations, (b) simulations with anthropogenic and natural forcing (ALL), (c) simulations with greenhouse gas changes only (GHG), and (d) simulations with aerosol changes only (AER). Trends are shown in grid cells in which at least 100 annual means are present, and grid cells are shown in grey otherwise. Equivalent trends calculated from the NAT simulations are small everywhere.

forcings present, we therefore regress the observations onto the ALL, GHG and NAT responses, and transform the resulting regression coefficients [Allen and Tett, 1999] to obtain scaling factors on the model's greenhouse gas (GHG), other anthropogenic (dominated by aerosols; OTH), and natural (NAT) responses. Decadal mean temperature anomalies were projected onto T4 spherical harmonics, and an EOF truncation of 30 was applied. We apply the detection and attribution analysis over the 1851–2010 period, which is longer than the typical period over which such analyses are applied [e.g., Hegerl *et al.*, 2007]. Since we have only 1280 years of control simulation available, we use anomalies relative to each ensemble mean [Stone *et al.*, 2007] to estimate the EOFs used in the truncation.

[9] Applying such an analysis over the 1851–2010 period, we find that the GHG, OTH and NAT responses are all detectable, since their regression coefficients are inconsistent with zero (first set of bars in Figure 3a). However, the responses to all three sets of forcings appear to be significantly overestimated by the model, since all three regression coefficients are significantly smaller than one. Such a picture would be consistent with the model having too high a Transient Climate Response (TCR): At 2.3°C its TCR would rank second highest amongst the CMIP3 models assessed by Randall *et al.* [2007]. The aerosol response has a particularly small best estimate regression coefficient of ~ 0.3 . Since the model's aerosol forcing itself is realistic (-0.8 W m^{-2} in 2005), this suggests that its response to aerosol forcing is too strong. Our focus here is mainly on the GHG regression coefficient, since this is the dominant factor scaling projected future warming. Over the period 1901–2000, similar to that used to derive the regression coefficients reported by Stott *et al.* [2006] and Hegerl *et al.* [2007], the best estimate of the greenhouse gas regression coefficient is considerably larger than that derived over the 1851–2010 period and consistent with one (third set of bars in Figure 3a). Figure 1a shows that the global mean temperature in the first two

decades of the 20th century was anomalously cool, while the decade 2001–2010, though warmer than the 1990s, exhibited less warming relative to the 1990s than the ALL simulations of CanESM2. Figure 3a shows that similar GHG regression coefficients to those derived over the period 1851–2010 are obtained either over the period 1851–2000 or 1901–2010. A similar but somewhat smaller sensitivity of the GHG regression coefficient to the period was seen in an analysis using the global mean only, with no signal-to-noise optimisation, and with anomalies expressed relative to a fixed 1901–2000 climatology. The uncertainty range on the GHG regression coefficient is found to be smaller in our analysis than that derived, for example, for HadCM3 by Stott *et al.* [2006] and Huntingford *et al.* [2006] using a similar analysis. This appears to relate to our use of a five-member ensemble rather than a four-member ensemble for all sets of simulations, our use of an EOF-basis derived from CanESM2 which results in a higher signal-to-noise ratio, and somewhat lower simulated internal variability in decadal mean temperature in CanESM2 compared to HadCM3. The OTH regression coefficient shows some sensitivity to the period, but differences are consistent with internal variability. The NAT regression coefficient is significantly larger for periods excluding the Krakatoa eruption, which would be consistent with the model having too strong volcanic forcing following Krakatoa [Joshi and Jones, 2009].

[10] The OTH and NAT regression coefficients are found to be somewhat sensitive to the EOF truncation used in the analysis, as shown in the fifth set of bars in Figure 3a, but the GHG regression coefficient is relatively insensitive to changes in truncation. Regression coefficients are relatively insensitive to the use of ALL, AER and NAT simulations in the regression (bars labelled AER), or to the use of intra-ensemble anomalies for estimating uncertainties (bars labelled ANOM). The last two sets of bars demonstrate that using global mean information only, while somewhat inflating uncertainties [Stott *et al.*, 2006] hardly changes

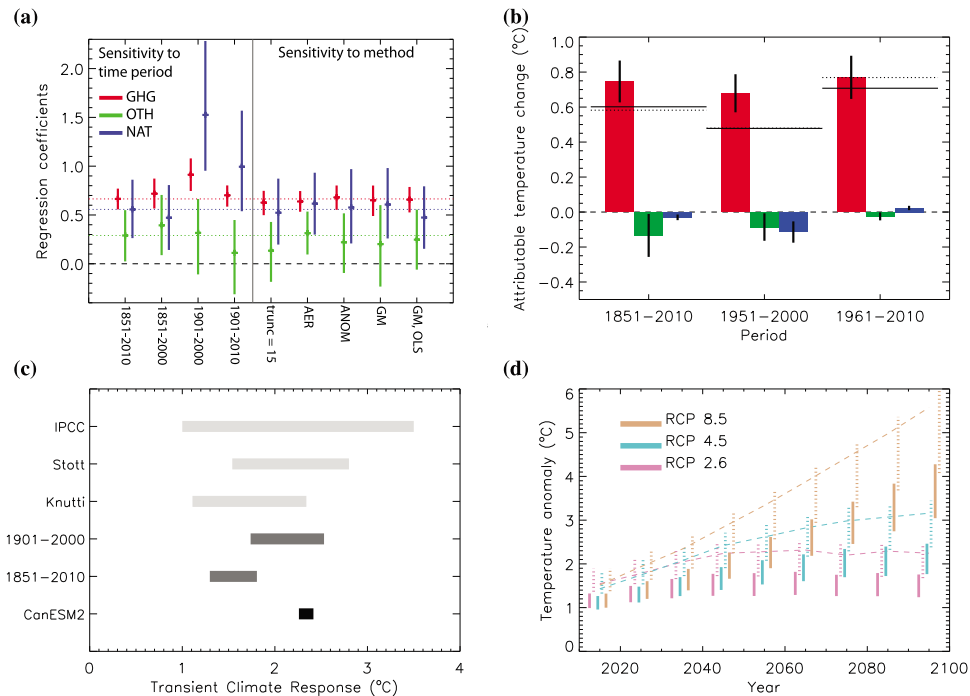


Figure 3. (a) Regression coefficients of observed temperature changes onto the simulated response to greenhouse gases (red), other anthropogenic forcings (green), and natural forcings (blue). The first set of bars, and the horizontal dotted lines, indicate the results from the standard case: a total least squares regression of 1851–2010 near-surface temperature anomalies projected onto T4 spherical harmonics, with an EOF truncation of 30, based on the ALL, GHG and NAT ensembles, and using intra-ensemble anomalies to estimate EOFs, and control to estimate uncertainties. The next three sets of bars show the sensitivity to the period. The remaining five sets of bars show results: derived using an EOF truncation of 15 ($\text{trunc} = 15$), based on the ALL, AER and NAT simulations (AER), derived using the control simulation to estimate EOFs, and intra-ensemble anomalies to estimate uncertainties (ANOM), based on the global mean temperature only (GM), and based on the global mean temperature, using an ordinary least squares regression and no signal-to-noise optimisation (GM, OLS). (b) Attributable temperature trends due to each set of forcings over each of the periods indicated in °C, based on the standard regression over the 1851–2010 period, with their associated uncertainties (vertical black lines). Horizontal dashed black lines indicate the sum of the trends attributable to each forcing, and horizontal solid lines indicate observed trends. (c) Transient Climate Response directly simulated by CanESM2 (black), constrained by observations using the 1851–2010 and 1901–2000 regressions (dark gray), and derived from observational constraints by *Stott et al.* [2006] (Stott), *Knutti and Tomassini* [2008] (Knutti), and *Hegerl et al.* [2007] (IPCC) (light gray). (d) Dashed lines show directly simulated global mean decadal mean temperature anomalies for each decade of the 21st century relative to the 1851–1860 mean for each RCP. Coloured bars show uncertainty ranges on observationally-constrained projections, derived by scaling projected GHG- and OTH-induced temperature changes using the 1851–2010 (solid) and 1901–2000 (dotted) GHG and OTH regression coefficients. All uncertainty ranges are 5–95%.

the best estimates of the regression coefficients, and similar regression coefficients are even derived based on the global mean using a simple ordinary least squares regression with no signal-to-noise optimisation. This demonstrates that the results do not depend strongly on the details of the analysis or the spatial patterns of the simulated responses. In all cases, a residual test [Allen and Tett, 1999] was passed at the 5% level, indicating consistency between regression residuals and simulated internal variability.

[11] Temperature trends attributable to each of the three sets of forcings considered were calculated over three periods by multiplying regression coefficients derived from the standard 1851–2010 case by trends simulated in response to each forcing over three different periods (Figure 3b). Over the period 1951–2000 our analysis indicates a smaller GHG-attributable warming, balanced by somewhat smaller OTH and NAT cooling than those shown by *Hegerl et al.* [2007] based on a 1900–1999 regression and other models. Over

the period 1961–2010, the OTH cooling is even smaller, due to the weaker simulated aerosol cooling over this period (Figure 1d), while natural forcings contributed a small warming over this period. Figure S1 in the auxiliary material shows equivalent regression coefficients and attributable warming derived from the CNRM-CM5 model.¹ Principal findings are broadly consistent: A lower greenhouse gas regression coefficient is derived using 1851–2010 data than using 1901–2000 data, this regression coefficient is more closely constrained when using data to 2010, and the best estimate of 1851–2010 greenhouse gas-attributable warming (important for scaling projections and TCR) differs by only 10%. However, uncertainties in this attributable warming are approximately twice as large due primarily to higher multi-decadal climate variability in CNRM-CM5.

¹Auxiliary materials are available in the HTML. doi:10.1029/2011GL050226.

[12] The GHG regression coefficient may also be used to estimate the Transient Climate Response by scaling the temperature response at the time of doubling CO₂ (averaged between the year 60 and 80) in a simulation with a 1% increase in CO₂ per year following *Stott et al.* [2006]. Uncertainties are derived by adding the uncertainty in the GHG regression coefficient and the sampling uncertainty in a 20-yr mean temperature in quadrature. Figure 3c indicates that the estimate of TCR derived based on the standard 1851–2010 regression is lower and more tightly constrained than when based on the 1901–2000 regression period typically used. These estimates of TCR are consistent with previously derived ranges (grey bars) [*Hegerl et al.*, 2007; *Knutti and Tomassini*, 2008; *Stott et al.*, 2006], though our ranges are more tightly constrained, in part because they are derived from a single model with relatively low multi-decadal variability and do not account for model uncertainty. Finally, the GHG and OTH regression coefficients may be used to obtain observationally-constrained projections of 21st century temperature following *Stott et al.* [2006]; This method is likely to be reliable for RCP 8.5, but could introduce errors for the stabilisation scenario RCP 2.6 of order 30% by the end of the century [*Kettleborough et al.*, 2007]. Both greenhouse gases and aerosol changes contribute warming during the 21st century, since sulphur dioxide emissions decline progressively under all RCP scenarios, thus scaling both components by the 1851–2010 regression coefficients reduces the amplitudes of both GHG-induced and aerosol-induced warming. Figure 3d shows that the observationally-constrained projections of 21st century temperature anomalies are markedly lower than those simulated directly by the model [*Arora et al.*, 2011] when the 1851–2010 regression coefficients are used to scale the projections. By contrast, when regression coefficients calculated over the shorter 1901–2000 period following [*Stott et al.*, 2006] are used to scale projections, projected warming is larger and consistent with that directly simulated, illustrating the sensitivity of the results to the regression period used.

4. Discussion and Conclusions

[13] Consistent with *Hegerl et al.* [2007], we detect a response to changes in greenhouse gases, aerosols and natural forcings in the full 1851–2010 instrumental temperature record, and find that greenhouse-gas-induced warming was significantly larger than the observed warming over the 1951–2000 period, partly balanced by cooling induced by aerosols and natural forcings. However, our estimate of GHG-attributable warming is both lower and more tightly constrained than that derived using data from the 20th century only. This results in an estimate of TCR of 1.3–1.8°C, which is towards the lower end of the observationally-constrained range assessed by *Hegerl et al.* [2007]. Our observationally-constrained estimates of 21st warming under the RCPs are also relatively tightly constrained and substantially lower than the warming simulated directly by CanESM2 [*Arora et al.*, 2011], with an overall projected range for global mean warming of the decade 2091–2100 relative to preindustrial of 1.2–4.3°C across the three RCPs.

[14] We have demonstrated that the lower and more tightly constrained GHG regression coefficient than that previously reported [*Huntingford et al.*, 2006; *Stott et al.*, 2006] results in part from our use of instrumental data

from a longer period beginning in 1851 and ending in 2010, and we have shown that our results derived using CanESM2 are robust to the details of the analysis. However, our results imply that CanESM2 overestimates the response to greenhouse gases, natural forcings, and particularly aerosols, and we find that its multi-decadal internal climate variability is lower than that in other models. We therefore recommend caution in interpreting the scaled projections derived from this single model, since our uncertainty estimates account only for possible errors in the magnitude of the simulated responses to the forcings, and not for possible errors in the observations, in the forcings, or in the spatio-temporal patterns of response to those forcings. We suggest that a similar analysis be carried out using multiple models once the necessary simulations are available, which will allow the effects of model uncertainty to be better accounted for.

[15] **Acknowledgments.** The authors thank Francis Zwiers and John Fyfe for their helpful comments on the manuscript.

[16] The Editor thanks the anonymous reviewers for assistance in evaluating this paper.

References

- Allen, M. R., and S. F. B. Tett (1999), Checking for model consistency in optimal fingerprinting, *Clim. Dyn.*, *15*, 419–434.
- Allen, M. R., P. A. Stott, J. F. B. Mitchell, R. Schnur, and T. L. Delworth (2000), Quantifying the uncertainty in forecasts of anthropogenic climate change, *Nature*, *407*, 617–620.
- Arora, V. K., J. F. Scinocca, G. J. Boer, J. R. Christian, K. L. Denman, G. M. Flato, V. V. Kharin, W. G. Lee, and W. J. Merryfield (2011), Carbon emission limits required to satisfy future representative concentration pathways of greenhouse gases, *Geophys. Res. Lett.*, *38*, L05805, doi:10.1029/2010GL046270.
- Brohan, P., J. J. Kennedy, I. Harris, S. F. B. Tett, and P. D. Jones (2006), Uncertainty estimates in regional and global observed temperature changes: A new data set from 1850, *J. Geophys. Res.*, *111*, D12106, doi:10.1029/2005JD006548.
- Hegerl, G. C., et al. (2007), Understanding and attributing climate change, in *Climate Change 2007: The Physical Science Basis*, edited by S. Solomon et al., chap. 9, pp. 663–745, Cambridge Univ. Press, Cambridge, U. K.
- Huntingford, C., P. A. Stott, M. R. Allen, and F. H. Lambert (2006), Incorporating model uncertainty into attribution of observed temperature change, *Geophys. Res. Lett.*, *33*, L05710, doi:10.1029/2005GL024831.
- Joshi, M. M., and G. S. Jones (2009), The climatic effects of the direct injection of water vapour into the stratosphere by large volcanic eruptions, *Atmos. Chem. Phys.*, *9*, 6109–6118.
- Kettleborough, J. A., B. B. Booth, P. A. Stott, and M. R. Allen (2007), Estimates of uncertainty in predictions of global mean surface temperature, *J. Clim.*, *20*, 843–855.
- Knutti, R., and L. Tomassini (2008), Constraints on the transient climate response from observed global temperature and ocean heat uptake, *Geophys. Res. Lett.*, *35*, L09701, doi:10.1029/2007GL032904.
- Meehl, G. A., et al. (2007), Global climate projections, in *Climate Change 2007: The Physical Science Basis*, edited by S. Solomon et al., chap. 10, pp. 747–845, Cambridge Univ. Press, Cambridge, U. K.
- Moss, R. H., et al. (2010), The next generation of scenarios for climate change research and assessment, *Nature*, *463*, 747–756.
- Randall, D. A., et al. (2007), Climate models and their evaluation, in *Climate Change 2007: The Physical Science Basis*, pp. 589–662, Cambridge Univ. Press, Cambridge, U. K.
- Stone, D. A., M. R. Allen, F. Selten, M. Kliphuis, and P. A. Stott (2007), The detection and attribution of climate change using an ensemble of opportunity, *J. Clim.*, *20*, 504–516.
- Stott, P. A., and J. A. Kettleborough (2002), Origins and estimates of uncertainty in predictions of twenty-first century temperature rise, *Nature*, *416*, 723–726.
- Stott, P. A., J. F. B. Mitchell, M. R. Allen, T. L. Delworth, J. M. Gregory, G. A. Meehl, and B. D. Santer (2006), Observational constraints on past attributable warming and predictions of future global warming, *J. Clim.*, *19*, 3055–3069.

V. K. Arora, G. M. Flato, N. P. Gillett, J. F. Scinocca, and K. von Salzen, Canadian Centre for Climate Modelling and Analysis, Environment Canada, PO Box 3065, STN CSC, Victoria, BC V8W 3V6, Canada. (nathan.gillett@ec.gc.ca)